Clinical Chemistry 50:9
1535–1543 (2004)

Molecular Diagnostics and Genetics

Detection of Genetic Variants of Transthyretin by Liquid Chromatography–Dual Electrospray Ionization Fourier-Transform Ion-Cyclotron-Resonance Mass Spectrometry

Angelito I. Nepomuceno,[1,4] Christopher J. Mason,[1] David C. Muddiman,[1,2*] H. Robert Bergen III,[1] and Steven R. Zeldenrust[3]

Background: **One of the numerous proteins causing amyloidosis is transthyretin (TTR), a protein usually responsible for the transport of thyroxine and retinol-binding protein. Variants within TTR cause it to aggregate and form insoluble fibers that accumulate in tissue, leading to organ dysfunction.**

Methods: **TTR was immunoprecipitated from serum by use of a polyclonal antibody and subsequently reduced with tris(2-carboxyethyl)phosphine. The purified TTR was then analyzed by fast-gradient liquid chromatography–dual-electrospray ionization Fourier-transform ion-cyclotron-resonance (FT-ICR) mass spectrometry. DNA sequencing was performed on all samples used in this study.**

Results: **Because of the inherent limitations in achieving high mass measurement accuracy based on the most abundant isotopic mass, we applied a fitting procedure that allowed determination of monoisotopic mass. Wild-type TTR (mean molecular mass, 13 761 Da) and its associated variant forms could be distinguished because of the high molecular mass accuracy afforded by FT-ICR (≤3 ppm) except for instances involving isobaric species or when isotopic distributions overlapped significantly. The $[M + 11\,H^+]^{11+}$ charge state for all samples was used to determine the mass accuracies for both wild-type and variant forms of the protein. We correctly assigned seven of seven TTR variants. Moreover, using a combination of proteomic and genomic technologies, we discovered and characterized a previously unreported *cis* double mutation with a mass only 2 Da different from wild-type TTR. Furthermore, DNA sequencing of the TTR gene for all individuals in this study completely agreed with the intact protein measurements.**

Conclusions: **FT-ICR mass spectrometry has sufficient mass accuracy to identify genetic variants of immunoaffinity-purified TTR. We believe that 91% of known TTR variants could be detected by this technique.**

Amyloidosis is characterized by deposition of insoluble fibril deposits of normally soluble proteins, eventually leading to organ dysfunction or complete failure. Familial amyloidotic polyneuropathy (ATTR)[5] is a hereditary form of this disease in which the deposits are composed of the protein transthyretin (TTR). TTR is synthesized predominantly in the liver and is involved in the transport of thyroxine and retinol-binding protein. It circulates in the serum as a tetramer of four identical subunits, each with 127 amino acids and a mean mass of 13 761 Da *(1–3)*. Variants of TTR are associated with deposition of amyloid as early as the third or fourth decade, whereas wild-type TTR has been shown to form cardiac amyloid deposits in elderly individuals. More than 100 variants have been

[1] W.M. Keck FT-ICR Mass Spectrometry Laboratory, Mayo Proteomics Research Center, Rochester, MN.

Departments of [2] Biochemistry and Molecular Biology and [3] Hematology, Mayo Clinic College of Medicine, Rochester, MN.

[4] Department of Chemistry, Virginia Commonwealth University, Richmond, VA.

*Address correspondence to this author at: Medical Sciences Building 3-115, Mayo Clinic College of Medicine, 200 First Street SW, Rochester, MN 55905. Fax 507-284-9261; e-mail muddiman.david@mayo.edu.

Received February 21, 2004; accepted May 13, 2004.

Previously published online at DOI: 10.1373/clinchem.2004.033274

[5] Nonstandard abbreviations: ATTR, amyloidotic polyneuropathy; TTR, transthyretin; MS, mass spectrometry; ESI, electrospray ionization; FT-ICR, Fourier-transform ion-cyclotron resonance; MMA, mass measurement accuracy; IMC, internal mass calibrant; TCEP, tris(2-carboxyethyl)phosphine; SDS, sodium dodecyl sulfate; PTM, posttranslational modification; and DTT, dithiothreitol.

published, with the majority leading to amyloidosis *(4–6)*. Currently, biopsy of affected end-organs followed by histologic staining with Congo red is used to diagnose amyloidosis; amyloid-positive tissues are then immunostained to identify the amyloid-forming precursor protein. Should a biopsy reveal that a patient suffers from ATTR, liver transplantation is contemplated in younger patients in an effort to prevent further amyloid deposits by removing the source of the amyloid-forming precursor. Alternative treatments involving drugs that stabilize the native tetrameric conformation of TTR are currently being explored as well *(7)*.

Mass spectrometry (MS) has played a crucial role in proteomics because of the soft ionization techniques of electrospray ionization (ESI) *(8, 9)* and matrix-assisted laser desorption/ionization *(10, 11)*. Wada et al. *(12)* were the first to perform the analysis of tryptic fragments of TTR by MS. This spawned several other mass spectrometric approaches to analyze and catalog TTR for any variations that differ from the wild-type amino acid sequence *(6, 13–20)*.

Fourier-transform ion-cyclotron-resonance (FT-ICR) MS can achieve mass measurement accuracy [MMA; (observed mass − theoretical mass)/theoretical mass × 10^6] of ≤3 ppm if it can accurately measure the cyclotron frequency of the ions of interest. Changes in ion cyclotron frequency occur as a result of variations in magnetic field strength, ion population (space charge), trapping potentials, and excitation conditions *(21–24)*. Coulombic interactions between the ions themselves are known to cause systematic shifts in the observed cyclotron frequency, otherwise known as space-charge effects. There are two categories of space-charge effects that influence the observed cyclotron frequency. The more pronounced of the two is referred to as "global" space-charge effect and is commonly taken into account in FT-ICR calibration laws *(23–25)*. Systematic error also originates from "local" space-charge effects attributable to more subtle "indirect" coulombic mechanisms, as observed by Masselson et al. *(26)* and Flora et al. *(27)*. To achieve high MMA, these space-charge effects must be quantitatively, routinely, and confidently accounted for. Internal calibration effectively compensates for space-charge effects. Because the internal mass calibrant (IMC) and analyte experience identical conditions within the ICR, the global space-charge component can be accounted for in the calibration equation *(23, 24)*.

Hannis and Muddiman *(22)* were the first to report success in using a dual ESI source for FT-ICR MS, routinely detecting intact biological macromolecules at mass accuracies of 3 ppm. Flora et al. *(27)* demonstrated MMAs of ~3 ppm (99% confidence interval of the mean) with the use of a dual ESI source for internally calibrating product ions formed from a 15mer oligonucleotide by the use of sustained off-resonance irradiation collision dissociation at 4.7 Tesla. Our group has shown the applicability of a dual ESI source *(22, 27–34)*, has surmounted the limitations of the first-generation source *(35)*, and has successfully applied this second-generation source *(34–36)*. Other groups have recently adopted this general strategy to achieve high MMA in FT-ICR *(37–39)*.

Here we describe a "targeted" proteomics approach for the characterization and identification of TTR variants based on immunoprecipitation by rabbit anti-human TTR antibodies and accurate mass measurements. Both wild-type and variant TTR are isolated from the vast number of proteins in serum by immunoprecipitation with a polyclonal antibody. TTR variants are detected by accurate mass measurements using a dual ESI source for internal calibration.

Materials and Methods

MATERIALS

Glucagon, angiotensin I, bradykinin, acetonitrile, 2-propanol, formic acid, sodium chloride, sodium sulfate, sodium phosphate monobasic, sodium phosphate dibasic, and tris(2-carboxyethyl)phosphine (TCEP) were obtained from Sigma-Aldrich. All materials were used as received. Deionized water was further purified to 18 MΩ with a Barnstead Nanopure Infinity ultrapure water system.

PREPARATION OF TTR PROTEIN EXTRACTION FROM SERUM

The Institutional Review Board of the Mayo Clinic granted approval for the study, and peripheral blood samples were drawn after informed consent was obtained from each participant.

TTR was purified according to the method of Bergen et al. *(40)* with slight modifications as described here. Rabbit anti-human TTR antibodies (Dako Corp.) were coupled to POROS AL (PerSeptive Biosystems) medium by the "recycling method" according to the manufacturer's instructions. We mixed 50 μL of serum and 50 μL of phosphate-buffered saline (10 mmol/L phosphate, pH 7.4, 150 mmol/L NaCl) before adding 20 μL of resin suspension (anti-human TTR antibodies) in a Handee™ MiniSpin column (Pierce Biotechnology). The solution was then incubated for ~1.5 h to allow for binding of the TTR to the antibody resin. The column was then centrifuged and the resin washed twice with phosphate-buffered saline. The purified TTR protein was eluted from the resin by 20 μL of 0.1 mol/L glycine (pH 2.8) and collected in a microcentrifuge tube.

We reduced the TTR samples with TCEP, adding 2 μL of a 100 mmol/L solution to the purified sample (20 μL), which we then kept at room temperature for 15 min.

ONE-DIMENSIONAL POLYACRYLAMIDE GEL ELECTROPHORESIS

Immunoaffinity-purified TTR and diluted plasma were diluted 1:1 with Laemmli sample buffer [63 mmol/L Tris, 100 mL/L glycerol, 20 g/L sodium dodecyl sulfate (SDS), and 0.0025 g/L bromphenol blue; 2-mercaptoethanol was added to this solution to a final concentration of 50

mL/L]. The immunoaffinity-purified TTR was acidic; we therefore added 1 μL of 3 mol/L Tris (pH 8.3) to each sample before boiling all samples for 3 min and then applying them to a 15% Tris-HCl Criterion precast gel (Bio-Rad). Tris/glycine running buffer (25 mmol/L Tris, 192 mmol/L glycine, 1 g/L SDS, pH 8.3) was used to run the gel for 0.9 h at 200 V. The gels were washed three times with water and then stained with Bio-Safe Coomassie G250 stain (Bio-Rad). After destaining with water, the gels were scanned with a GS800 densitometer (Bio-Rad). Protein molecular mass markers were included for reference.

MS

Mass spectra were obtained with a modified ESI-FT-ICR mass spectrometer (IonSpec) equipped with an actively shielded 7-Tesla superconducting magnet (Cryomagnetics). The ESI source (Analytica, Branford) was modified to accept a heated metal capillary *(41)* and a new dual ESI source *(35)* and has been described elsewhere in detail *(34, 35)*. Software for calculation of monoisotopic mass using an algorithm described by Senko et al. *(42)* was written in C++ in Linux. Theoretical isotopic distributions were generated with the Mercury algorithm *(43)*.

Nano-LC-MS of TTR

The chromatography system consisted of two Shimadzu LC-10ADvp pumps with an SCL-10Avp controller (flow rate was adjusted by splitting to give ~500 nL/min through the column). Solvent A was water–acetonitrile (95:5 by volume) containing 2 g/L formic acid; solvent B was water–acetonitrile (5:95 by volume) containing 2 g/L formic acid. A third LC-10ADvp pump [methanol–water (10:90 by volume) containing 0.1 g/L trifluoroacetic acid; 30 μL/min] was used to load the TTR sample on a C_4 trap. The trap consisted of a LC Packings micro precolumn (0.3 × 5 mm) packed with Magic C_4 (300 Å pore size, 5-μm bead diameter; Michrom Bioresources, Inc.).

The C_4 trap was plumbed into a 10-port valve (Cheminert; VICI Valco Instruments). In position A the sample was injected and loaded on the C_4 trap with the sample-loading pump. In position B, the trap was in-line with the nano-LC column and the analyte was eluted off the trap with an organic gradient. The gradient profile for eluting TTR from the C_4 trap was 0–3 min held at 5% B, 3–6 min linearly ramped to 60% B, 6–9 min held at 60% B, and 9–10 min linearly ramped to 95% B.

Data acquisition began simultaneously with the start of the LC gradient. The total hexapole accumulation time for both the internal standard and apomyoglobin digest was 2000 ms; 250 ms were spent on the IMC emitter, and the remaining 1750 ms were spent on the eluate from the nano-LC column. The IMC consisted of a 2 μmol/L solution of angiotensin I, bradykinin, and/or glucagon, which was infused directly through a second emitter at a flow rate of 300 nL/min while the LC effluent was sprayed through the primary emitter during the LC-MS run. Each mass spectrum was internally calibrated by use of the monoisotopic peaks that directly flanked the $[M + 11H^+]^{11+}$ charge state of the wild-type and variant proteins.

Gene sequencing

High-quality genomic DNA was isolated from peripheral blood buffy coat by use of DNAzol (Invitrogen). Further details can be found elsewhere *(40)*.

Results and Discussion

Analysis of wild-type sequence

The presence of posttranslational modifications (PTMs) of TTR may have some role in promoting amyloid fibril formation by variant forms of TTR. The more commonly associated PTMs are the conjugation of cysteine, sulfonate (SO_3H), cysteinylglycine, or glutathione to the lone cysteine of the wild-type sequence. Kishikawa et al. *(16)* have stated that the S-sulfonated species can be used as a marker for identifying patients with molybdenum cofactor deficiency, a fatal neurologic disorder. Supportive evidence by Sass et al. *(44)* has also shown that the identification of an uncommon *S*-homocysteinylation adduct may be useful in understanding hyperhomocysteinemia-related diseases. Several groups are currently pursuing the importance of TTR PTMs. However, the ability to identify variants can be compromised by the presence of these PTMs. Removal of Cys adducts allows accurate analysis of TTR variants by preventing overlapping isotopic distributions between the wild type, variants, and their respective PTMs.

The purity of the immunoaffinity-purified TTR relative to plasma is shown in the one-dimensional polyacrylamide gel (Fig. 1, top left). The immunoaffinity-purified TTR was composed primarily of TTR with some higher-molecular-mass contaminants that did not affect the analysis. The arrow indicates the band corresponding to TTR at ~13.7 kDa. A typical multiply charged spectrum of TTR immunoaffinity purified by our method is shown in Fig. 1. The TTR spectrum overwhelms the underlying noise, which may be a result of the high-molecular-mass species shown in the gel. Additionally, a total-ion chromatogram indicated a single chromatographic peak that is specific to TTR [see Fig. 6 in Bergen et al. *(40)*, which appears in this issue]. Although the bands on the gel indicate the presence of other proteins, they did not interfere with obtaining a "clean" spectrum of TTR that was easy to interpret (Fig. 1).

The spectrum in Fig. 1 is a LC-dual-ESI-FT-ICR mass spectrum of the immunopurified TTR from a patient diagnosed with ATTR. DNA sequencing verified that a transversion mutation of the DNA sequence produced a G47E variant in the amino acid sequence (data not shown). The broadband spectrum illustrates that there are two forms of TTR present: wild type and a variant form (G47E) producing a +72 Da intact molecular mass shift. The scan shown in the inset (top right) in Fig. 1 further

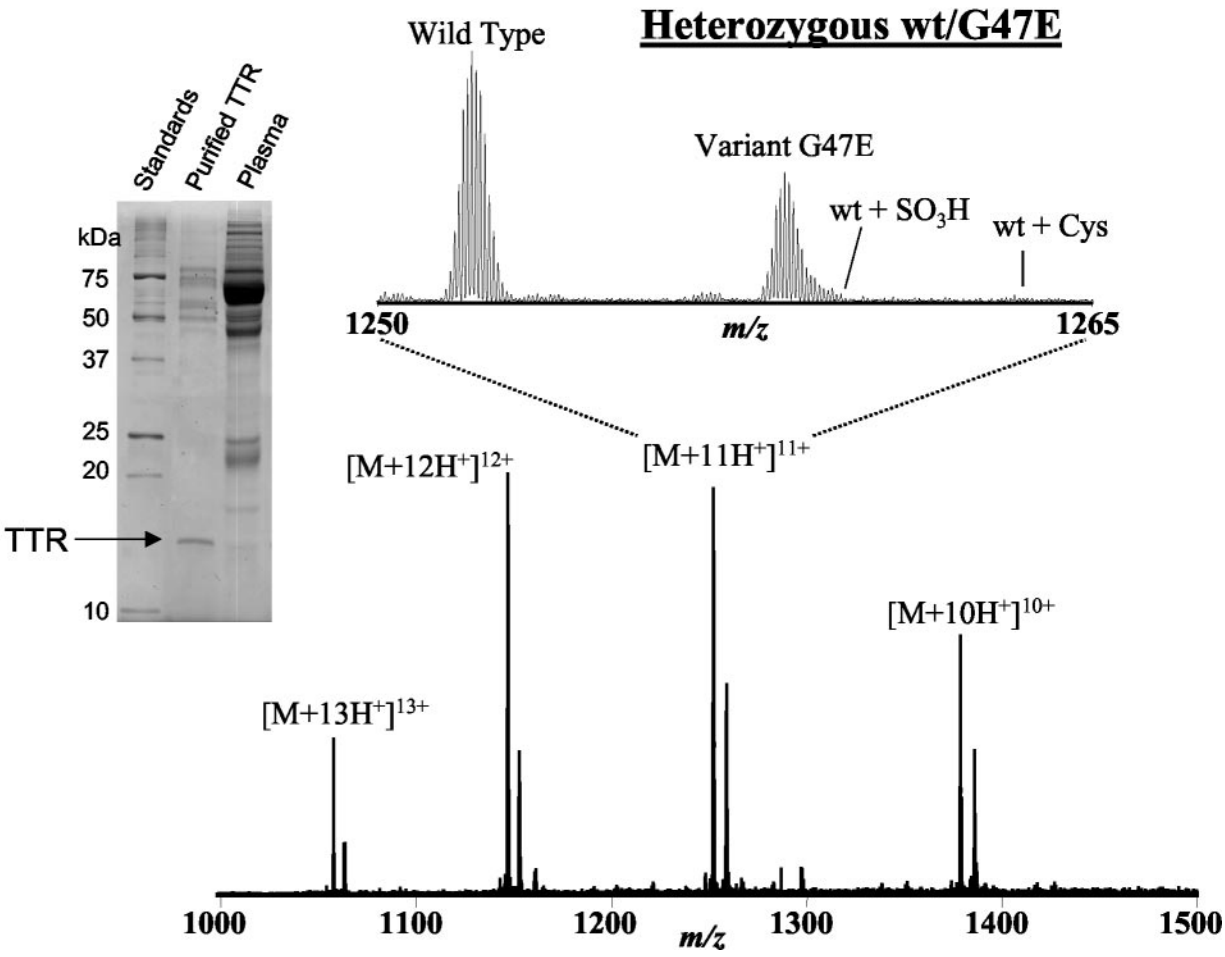

Fig. 1. Analysis of TTR from a heterozygous wild-type/G47E patient.

The inset (*top left*) shows a one-dimensional SDS-polyacrylamide gel of immunoaffinity-purified TTR (*center lane*) and diluted plasma (*right lane*) for comparison. A single-acquisition ESI-FT-ICR mass spectrum of TTR derived from the patient is shown at the *bottom*. This TTR was reduced with TCEP. The expansion plot (*top right*) shows the $[M + 11H^+]^{11+}$ charge state for both the wild-type (*wt*) and variant proteins and indicates where common wild-type TTR adducts would be found in the spectrum.

demonstrates the effectiveness of using a reducing agent that makes the G47E variant readily distinguishable from cysteine adducts. The simplification of the mass spectrum of TTR is afforded by reduction, which can also be seen in Bergen et al. *(40)*.

We considered using TCEP for reduction because of the low pH matrix (pH 2.7) needed to elute the TTR from the antibody resin. Getz et al. *(45)*, who compared the reduction achieved with TCEP and dithiothreitol (DTT) for use in protein biochemistry, showed compelling evidence for the use of TCEP over DTT. Han and Han *(46)* reported that TCEP is a more effective reducing agent than DTT at lower pH values. Fig. 1 is an example of a TTR sample that was reduced by use of TCEP before analysis; no residual adducts can be detected. An added advantage of using TCEP was the time needed for reduction of TTR. A total of 15 min was required, compared with the 1.5 h needed for reduction by DTT (data not shown). The short reduction time facilitates high-throughput screening of TTR variants.

The total analysis time for a single measurement, as depicted in Fig. 1, is ~10 min and is largely a result of reestablishing the gradient. However, in a clinical environment, column-switching techniques could be used, which would reduce this time. Furthermore, decoupling the LC concentration/desalting step would allow use of flow-injection analysis requiring <30 s per sample.

DETERMINATION OF VARIANTS BY USE OF ACCURATE MASS MEASUREMENTS

Comparison of accurate mass measurements of proteins with theoretical masses can reveal the presence of genetic variants. Although the most abundant isotopic mass of a protein or peptide is readily detectable experimentally, it may differ by up to 1 Da from the theoretical mass of the most abundant isotopic species because of the experimental variability of ion abundances *(47)*. Monoisotopic mass is preferred for comparison because it is not subject to this uncertainty and because it does not depend on the characteristics of the isotopic distribution, which varies with

mass. However, the monoisotopic masses of molecules larger than 5 kDa have extremely low abundance and are therefore not readily detected. In the present study, experimental monoisotopic masses were determined by an isotope-fitting procedure using the χ^2 statistic as our metric for the best fit. This approach, first described by Senko et al. *(42)*, aligns a theoretical isotopic distribution to the experimental isotopic distribution. Several possible distribution alignments are obtained by shifting the theoretical isotopic distribution in $\sim 1/z$ increments relative to the experimental distribution.

For each possible alignment, a χ^2 value between experimental and theoretical abundances was calculated. Only pairs of peaks in which the experimental abundance was >20% of the most abundant isotopic peak in the distribution were included. The alignment with the lowest χ^2 value was taken to be optimal. The monoisotopic mass for each isotopic peak was then calculated by an abundance-weighted average of differences between experimental mass and theoretical monoisotopic mass *(48)*. This procedure will be referred to as targeted isotopic fitting.

Whereas Senko et al. *(42)* used a model amino acid, averagine, whose chemical composition was obtained by averaging the relative occurrence of each amino acid in a database, we used the known amino acid composition of the wild-type protein to produce the theoretical distribution. The specificity of the antibody used for immunopurification of TTR before analysis ensured that the chemical composition of the experimental species closely resembled the wild type. Genetic variants obviously change the chemical composition and will therefore change the isotopic distribution, but, at least in the case of substitutions or small insertions and deletions, this change does not affect the targeted isotopic fitting procedure.

An expanded region of the $[M + 11H^+]^{11+}$ charge state for a mass spectrum that was acquired by LC-dual-ESI-FT-ICR is shown in Fig. 2. The 11+ charge state was selected as it was typically the most abundant charge state

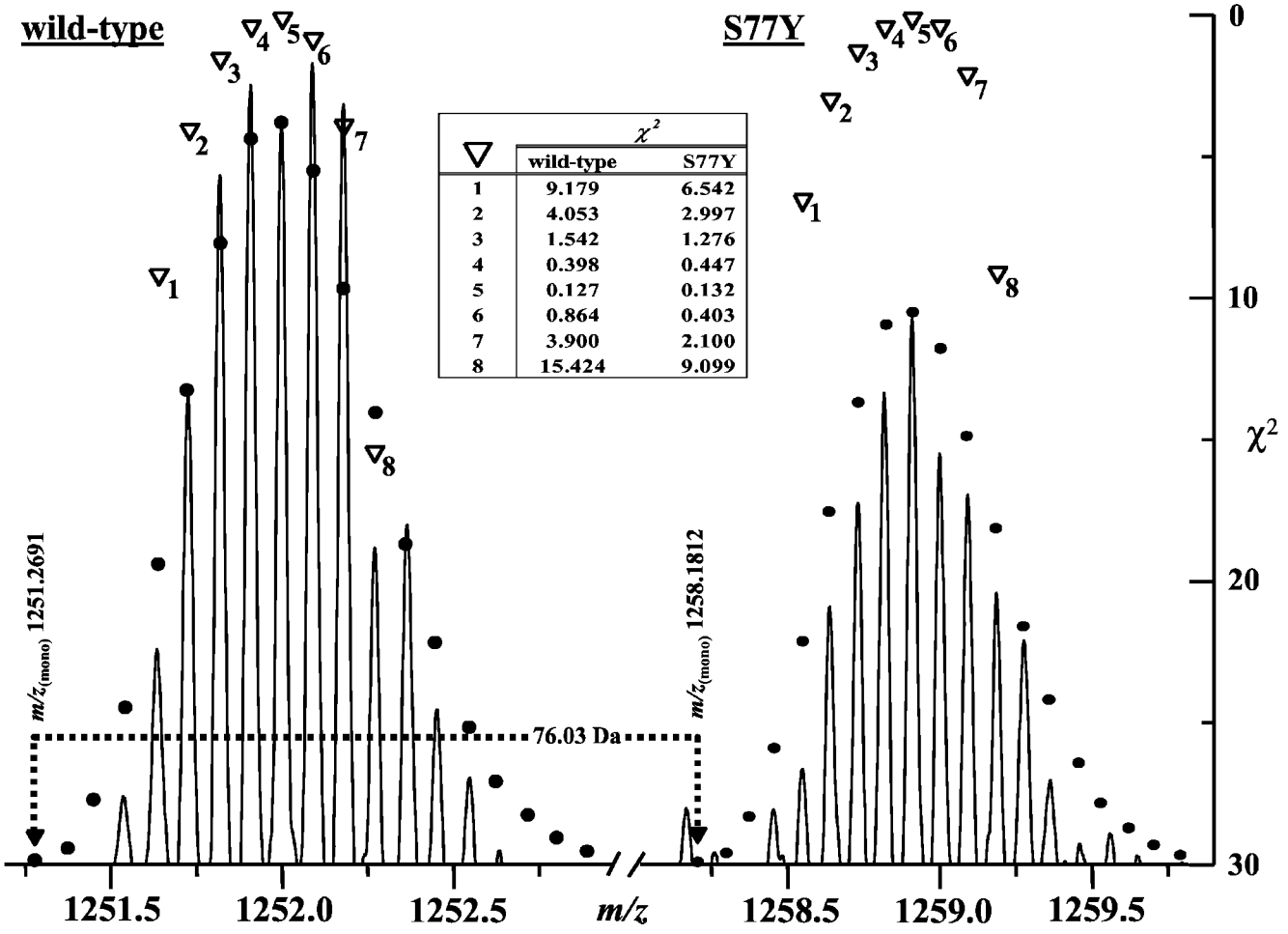

Fig. 2. Expansion plot of a single-acquisition ESI-FT-ICR mass spectrum of TTR isolated from a heterozygous wild-type/S77Y patient.

The isotopic resolutions of the wild-type (*left*) and variant (*right*) proteins of $[M + 11H^+]^{11+}$ charge state are shown. ● indicate theoretical isotopic distributions for both the wild-type and variant proteins. The values of the χ^2 statistic (▽) for various alignments are shown; the lower χ^2 values (*table between distributions*) indicate better alignment (axis is inverted). The *arrows* at 1251.2691 and 1258.1812 Da indicate the abundance-weighted monoisotopic masses of the wild type and S77Y variant (note that the peak near the variant monoisotopic mass is a noise peak, not the monoisotopic species).

and was bracketed by the IMCs. In Fig. 2, two separate experimental isotopic distributions are observed; one corresponding to wild type (MMA = 0.6 ppm), the other clearly indicating the presence of a variant. The filled circles represent the theoretical isotopic distribution for this multiply charged ion, whereas the open inverted triangles show the value of the χ^2 statistic for a variety of alignments. The arrow for each distribution represents the calculated monoisotopic *m/z* values. The calculated experimental monoisotopic mass is then compared with a table of theoretical monoisotopic masses for known TTR variants. In this case, the calculated neutral monoisotopic mass (13 828.914 Da) corresponded well to the theoretical neutral monoisotopic mass of the S77Y variant (13 828.920 Da), giving a MMA of 0.4 ppm. DNA sequencing data were also used to verify that this was a S77Y variant (data not shown).

The results for seven individuals who were screened and tested positive for TTR variants are shown in Table 1. Indicated in Table 1 are the neutral monoisotopic masses and the resulting mass errors. Once we had determined that a variant was present, we performed DNA analysis to confirm the results (data not shown). The mean MMA achieved for all seven samples was −0.21 ± 1.2 ppm (mean ± confidence interval of the mean at the 95% confidence level) for variant forms. Six of the seven individuals were heterozygous; the mean MMA achieved for the wild-type protein was −0.48 ± 2.26 ppm (0.01 ± 0.03 Da mass error). In comparison, Bergen et al. *(40)*, using a low-resolution single-quadrupole instrument, obtained an intraassay mass difference of −28.1 (0.3) Da [mean (SD)] for a Val94Ala variant measured 10 times the same day and an interassay comparison of 28.7 (0.2) Da for the same sample measured 5 times on day 5. When 49 wild-type TTR samples were analyzed on the same day, Bergen et al. *(40)* obtained a mean mass of 13 761.5 ± 0.2 Da (mean ± confidence interval of the mean) at the 95% confidence level using the same low-resolution MS. Only the FT-ICR instrumentation provided the requisite high resolving power and mass accuracy to ascertain the mass differences of TTR containing a ≥2 Da mass shift, whereas the instrument with lower resolving power detected variants with mass shifts ≥10 Da *(40)*.

Of the >90 known TTR genetic variants, it is possible that 8 variants would give a false-negative outcome. Two of the eight are isobaric (i.e., I ↔ L or Q ↔ K) with the wild type and would not be distinguished by mass spectrometric screening methods. The remaining six differ from the wild-type molecular mass by 1 Da. Identifying individuals homozygous for any ±1 Da variant becomes a feasible task because of the high MMA achieved. However, a majority of the individuals who have been diagnosed with ATTR are heterozygous, suggesting that there would be two forms of the protein, a wild type as well as the protein variant (± 1 Da). A mass-resolving power ($m/\Delta m$) of >300 000 (full-width half-maximum; FWHM) must be achieved to distinguish the overlapping isotopic distributions from the wild-type and variant TTR proteins (e.g., to resolve the monoisotopic mass of a +1 Da variant from the wild-type protein with one ^{13}C incorporated into it Δm would need to be <0.05 Da). The typical resolving power obtained using the experimental conditions stated earlier was $\sim 35\,000_{FWHM}$.

The remaining 82 genetic variants (91%) can be unambiguously detected based on mass. However, some variants are isobaric with each other, and the location of the variant cannot be determined from intact accurate mass measurements alone. Of the 82 variants, 27 (33%) can be conclusively located. Determining the site of the remaining 55 isobaric variants (77%) could be important to correlate with disease progression.

DETECTION OF NOVEL *CIS* DOUBLE MUTATION

The $[M + 11H^+]^{11+}$ charge state of a theoretical wild-type isotopic distribution and an experimental isotopic distribution are shown in Fig. 3A. The single experimental isotopic distribution in this spectrum was first assumed to be wild type. However, the neutral monoisotopic mass was calculated to be 13 753.882 Da (72 ppm MMA when compared with the theoretical wild-type neutral monoisotopic mass of 13 752.887 Da), which is significantly outside of our achievable limits (± 3 ppm) using the dual ESI

Table 1. Results for seven individuals positive for TTR variants.

Sample	Protein mutation	Confirmed DNA mutation[a]	Nominal mass shift (Da)	Monoisotopic neutral mass,[b] Da		Error, Da	MMA,[c] ppm
				Observed	Theoretical		
A	G6S	GGT→AGT	+30	$13\,782.91_4$	$13\,782.89_9$	0.02	1.1
B	T60A	ACT→GCT	−30	$13\,722.86_7$	$13\,722.87_8$	−0.01	−0.8
C	G6S	GGT→AGT	+30	$13\,782.92_7$	$13\,782.89_9$	0.03	2.0
D	E54G	GAG→GGG	−72	$13\,680.84_6$	$13\,680.86_7$	−0.02	−1.5
E	S77Y	TCT→TAT	+76	$13\,828.91_4$	$13\,828.92_0$	−0.01	−0.4
F	G47E	GGG→GAG	+72	$13\,824.88_9$	$13\,824.90_9$	−0.02	−1.4
G	S77Y	TCT→TAT	+76	$13\,828.91_4$	$13\,828.92_0$	−0.01	−0.4

[a] Underlined bases indicate the affected nucleotides.
[b] Monotopic neutral mass calculation: $(m/z_{mono} \times z) - (z \times H^+)$.
[c] Mean MMA = −0.21 ± 1.2 (confidence interval of the mean at 95% confidence level) ppm.

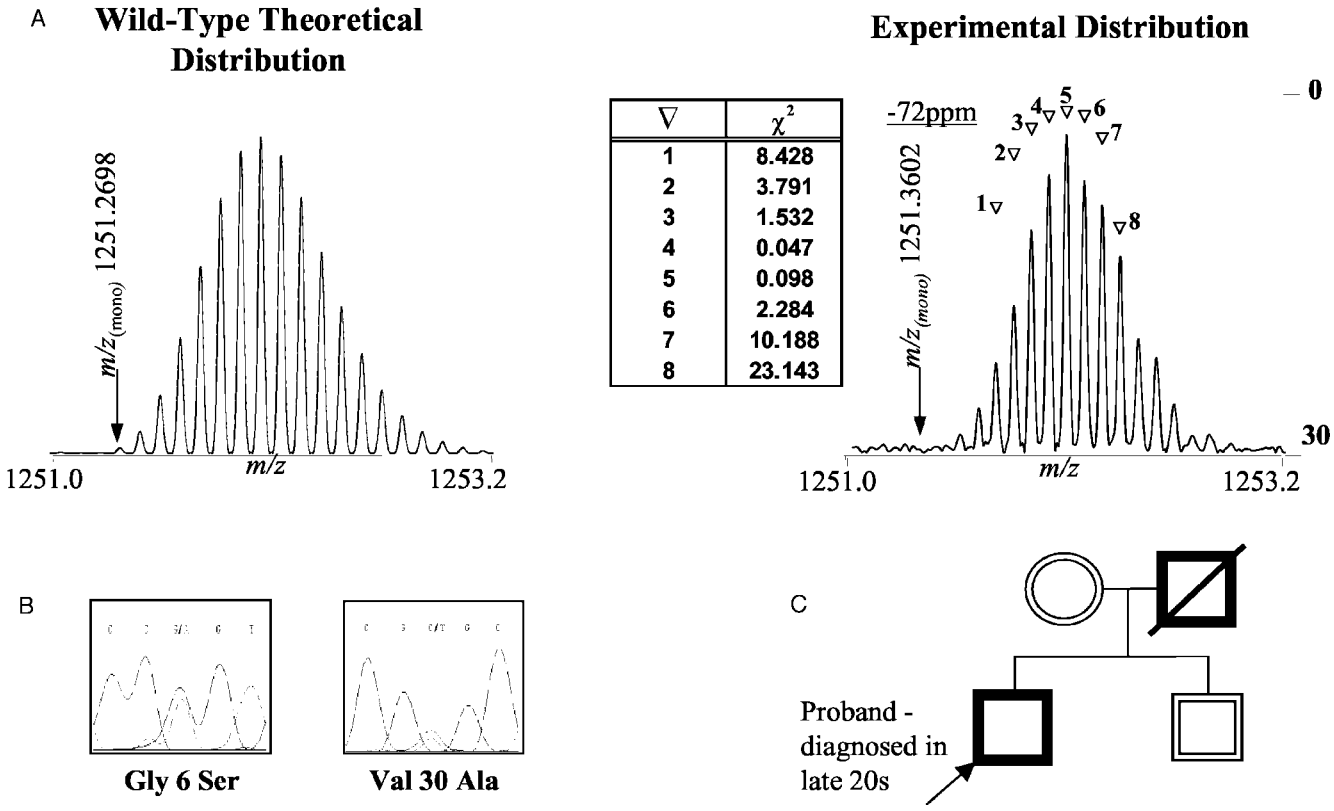

Fig. 3. Isotopic distributions of the $[M + 11H^+]^{11+}$ charge state for theoretical wild-type TTR and for a wild-type/*cis* (G6S & V30A) individual.

(*A*), the theoretical isotopic distribution of the $[M + 11H^+]^{11+}$ charge state wild-type TTR is shown on the *left*. An expansion plot of the $[M + 11H^+]^{11+}$ charge state derived from a single-acquisition ESI-FT-ICR mass spectrum of TTR isolated from a patient who was initially thought to be homozygous wild type is shown on the *right*. Indicated are both the theoretical and calculated isotopic distributions and their respective monoisotopic *m/z* values. The value of the χ^2 statistic (▽) is shown for various alignments; the lower χ^2 values (*table between distributions*) indicate better alignment (axis is inverted). The corresponding MMA of −72 ppm was obtained working under the initial assumption that this individual was homozygous wild type. This poor MMA provided sufficient evidence that this individual is not wild type, warranting further investigation. (*B*), DNA sequencing results verifying that that this sample is not wild type but rather that two mutations were present (G6S & V30A). (*C*), two-generation family pedigree of the *cis* variant.

source for internal calibration and fitting the isotopic distribution to obtain monoisotopic mass. These data clearly suggested that this individual was not homozygous wild type. DNA sequencing (Fig. 3B) was performed to determine whether something other than an aberration in our methodology could explain this poor MMA. Indeed, the DNA sequencing data showed that there are two variants present in this particular individual, a G6S (+30 Da shift in protein mass) and a V30A (−28 Da shift in protein mass).

Because ATTR is a familial disease, it is important to know from whom the variant(s) originated. If a double mutation were to occur in *trans* (the maternal and paternal chromosome would each contain a single mutation), there would be two distinct isotopic distributions for each variant; however, this is not observed (Fig. 3A). If the mutations were to occur in *cis* (both mutations reside on the same chromosome), the resulting protein net mass shift would be +2 Da. If an individual is heterozygous, two isotopic distributions would be observed: one representing the wild type and the other the *cis* variant. The resolving power necessary to distinguish the wild type and the *cis* (G6S and V30A) variant is not typically achieved, providing a composite isotopic distribution, as observed (Fig. 3A). Additional work is continuing on computational methods to routinely determine the presence of significantly overlapping isotopic distributions. In particular, we are exploring the use of the figure-of-merit calculation from THRASH *(48)* in an examination of how the signal-to-noise ratio affects the limits of detection for admixtures of small mass shifts in proteins of appreciable molecular mass.

Although MMA did not uniquely identify the genetic variant present, the combination of DNA sequencing and mass spectrometric results clearly indicated that the individual is heterozygous wild type/*cis* (G6S and V30A). Fig. 3C shows the pedigree for the patient analyzed, the proband individual (index case) presented with typical ATTR symptoms in his late twenties. The immediate family (mother and brother) tested negative for the genetic variants of TTR. The father could not be tested because he is deceased, but his death had been attributed to amyloidosis. Because it is known that the mother was wild type, it can be concluded that the *cis* (G6S and V30A) variant originated from the paternal chromosome.

Double mutations are very rare: there has been only

one other report, by Ando et al. *(49)*, of an individual with a double TTR mutation. This particular finding showed that the individual carried a heterozygous *trans* variant. Ours is the first report of a *cis* double mutation of TTR. This particular *cis* double mutation was detected by a combination of genomic and proteomic approaches.

In conclusion, we used a targeted proteomics approach to characterize TTR variants by use of LC-dual-ESI FT-ICR MS. The high mass-resolving power translates into high MMA when an isotopic fitting procedure is used. Genetic variants of TTR can be detected effectively by use of quadrupole MS platforms *(40)*, but unambiguous results can be obtained for >91% of known TTR genetic variants when FT-ICR MS is used for detection. Identification of variants is achieved routinely and accurately because of the high MMA (<3 ppm) largely afforded by the high mass-resolving power, the dual ESI source, and the isotopic fitting procedure. Importantly, we could determine, with contributions from both protein analysis and DNA sequencing, that an individual was heterozygous wild type and *cis* (G6S and V30A) variant. This is the first report of an individual with a *cis* double variant.

We are grateful for the financial support of the NIH (Grant R01HG02159), The Hematology Malignancies Fund (Grant REF20P), The W.M. Keck Foundation, and the Mayo Clinic College of Medicine for the Medical Education and Research. We thank Dr. Alan Rockwood (ARUP Institute for Clinical and Experimental Pathology, Salt Lake City, UT) for providing us with the code for the Mercury algorithm.

References

1. Mita S, Maeda S, Shimada K, Araki S. Cloning and sequence analysis of cDNA for human prealbumin. Biochem Biophys Res Commun 1984;124:558–64.
2. Kanda Y, Goodman DS, Canfield RE, Morgan FJ. The amino acid sequence of human plasma prealbumin. J Biol Chem 1974;249:6796–805.
3. Blake CC, Geisow MJ, Swan ID, Rerat C, Rerat B. Structure of human plasma prealbumin at 2–5 Å resolution. A preliminary report on the polypeptide chain conformation, quaternary structure and thyroxine binding. J Mol Biol 1974;88:1–12.
4. Connors LH, Richardson AM, Theberge R, Costello CE. Tabulation of transthyretin (TTR) variants as of 1/1/2000. Amyloid Int J Clin Exp Invest 2000;7:54–69.
5. Saraiva MJ. Transthyretin mutations in hyperthyroxinemia and amyloid diseases. Hum Mutat 2001;17:493–503.
6. Theberge R, Connors LH, Skinner M, Costello CE. Detection of transthyretin variants using immunoprecipitation and matrix-assisted laser desorption/ionization bioreactive probes: a clinical application of mass spectrometry. J Am Soc Mass Spectrom 2000;11:172–5.
7. Klabunde T, Petrassi HM, Oza VB, Raman P, Kelly JW, Sacchettini JC. Rational design of potent human transthyretin amyloid disease inhibitors. Nat Struct Biol 2000;7:312–21.
8. Fenn JB, Mann M, Meng CK, Wong SF, Whitehouse CM. Electrospray ionization for mass spectrometry of large biomolecules. Science 1989;246:64–71.
9. Fenn JB, Mann M, Meng CK, Wong SF, Whitehouse CM. Electrospray ionization-principles and practice. Mass Spectrom Rev 1990;9:37–70.
10. Tanaka K, Waki H, Ido Y, Akita S, Yoshida Y, Yoshida T. Protein and polymer analysis up to *m/z* 100 000 by laser ionization time-of-flight mass spectrometry. Rapid Commun Mass Spectrom 1988;2:151–3.
11. Karas M, Hillenkamp F. Laser desorption ionization of proteins with molecular masses exceeding 10 000 Daltons. Anal Chem 1988;60:2299–301.
12. Wada Y, Matsuo T, Katakuse I, Suzuki T, Azuma T, Tsujino S, et al. Mass spectrometric detection of the plasma prealbumin (transthyretin) variant associated with familial amyloidotic polyneuropathy. Biochim Biophys Acta 1986;873:316–9.
13. Theberge R, Connors L, Skinner M, Skare J, Costello CE. Characterization of transthyretin mutants from serum using immunoprecipitation, HPLC/electrospray ionization and matrix-assisted laser desorption/ionization mass spectrometry. Anal Chem 1999;71:452–9.
14. Lim A, Prokaeva T, McComb ME, O'Connor PB, Theberge R, Connors LH, et al. Characterization of transthyretin variants in familial transthyretin amyloidosis by mass spectrometric peptide mapping and DNA sequence analysis. Anal Chem 2002;74:741–51.
15. Nakanishi T, Okamoto N, Tanaka K, Shimizu A. Laser desorption time-of-flight mass spectrometric analysis of transferrin precipitated with antiserum: a unique simple method to identify molecular weight variants. Biol Mass Spectrom 1994;23:230–3.
16. Kishikawa M, Nakanishi T, Miyazaki A, Shimizu A, Nakazato M, Kangawa K, et al. Simple detection of abnormal serum transthyretin from patients with familial amyloidotic polyneuropathy by high-performance liquid chromatography/electrospray ionization mass spectrometry using material precipitated with specific antiserum. J Mass Spectrom 1996;31:112–4.
17. Kishikawa M, Sass JO, Sakura N, Nakanishi T, Shimizu A, Yoshioka M. The peak height ratio of S-sulfonated transthyretin and other oxidized isoforms as a marker for molybdenum cofactor deficiency, measured by electrospray ionization mass spectrometry. Biochim Biophys Acta 2002;1588:135–8.
18. Kiernan UA, Tubbs KA, Gruber K, Nedelkov D, Niederkofler EE, Williams P, et al. High-throughput protein characterization using mass spectrometric immunoassay. Anal Biochem 2002;301:49–56.
19. Yamashita T, Ando Y, Bernt Suhr O, Nakamura M, Sakashita N, Ohlsson PI, et al. A new diagnostic procedure to detect unknown transthyretin (TTR) mutations in familial amyloidotic polyneuropathy (FAP). J Neurol Sci 2000;173:154–9.
20. Ando Y, Ohlsson PI, Suhr O, Nyhlin N, Yamashita T, Holmgren G, et al. A new simple and rapid screening method for variant transthyretin-related amyloidosis. Biochem Biophys Res Commun 1996;228:480–3.
21. Easterling ML, Mize TH, Amster JI. Routine part-per-million mass accuracy for high mass ions: space charge effects in MALDI FT-ICR. Anal Chem 1999;71:624–32.
22. Hannis JC, Muddiman DC. A dual electrospray ionization source combined with hexapole accumulation to achieve high mass accuracy of biopolymers in Fourier transform ion cyclotron resonance mass spectrometry. J Am Soc Mass Spectrom 2000;11:876–83.
23. Jeffries JB, Barlow SE, Dunn GH. Theory of space-charge shift of ion cyclotron resonance frequencies. Int J Mass Spectrom Ion Process 1983;54:169–87.
24. Francl TJ, Sherman MG, Hunter RL, Locke MJ, Bowers WD, McIver

RT. Experimental determination of the effects of space charge on ion cyclotron resonance frequencies. Int J Mass Spectrom Ion Process 1983;54:189–99.
25. Ledford EB, Rempel DL, Gross ML. Space charge Effects in Fourier transform mass spectrometry. II. Mass calibration. Anal Chem 1984;56:2744–8.
26. Masselon C, Anderson GA, Harkewicz R, Bruce JE, Pasa-Tolic L, Smith RD. Accurate mass multiplexed tandem mass spectrometry for high-throughput polypeptide identification from mixtures. Anal Chem 2000;72:1918–24.
27. Flora JW, Hannis JC, Muddiman DC. High mass accuracy of product ions produced by SORI-CID using a dual electrospray ionization source coupled with FTICR mass spectrometry. Anal Chem 2001;73:1247–51.
28. Flora JW, Muddiman DC. Selective, sensitive, and rapid phosphopeptide identification in enzymatic digests using ESI-FTICR-MS with infrared multiphoton dissociation. Anal Chem 2001;73:3305–11.
29. Flora JW, Muddiman DC. Complete sequencing of mono-deprotonated peptide nucleic acids by sustained off-resonance irradiation collision-induced dissociation. J Am Soc Mass Spectrom 2001;12:805–9.
30. Chen S, Hannis JC, Flora JW, Muddiman DC, Charles K, Yu Y, et al. Homogeneous preparations of 3′-phosphoglycolate-terminated oligodeoxynucleotides from bleomycin-treated DNA as verified by electrospray ionization Fourier transform ion cyclotron resonance mass spectrometry. Anal Biochem 2001;289:274–80.
31. Null AP, Hannis JC, Muddiman DC. Genotyping of simple and compound short tandem repeat loci using electrospray ionization Fourier transform ion cyclotron resonance mass spectrometry. Anal Chem 2001;73:4514–21.
32. Null AP, George LT, Muddiman DC. Evaluation of sample preparation techniques for mass measurements of PCR products using ESI-FT-ICR mass spectrometry. J Am Soc Mass Spectrom 2002;13:338–44.
33. Hannis JC, Muddiman DC. Tailoring the gas-phase dissociation and determining the relative energy of activation for dissociation of 7-deaza modified oligonucleotides containing a repeating motif. Int J Mass Spectrom Ion Process 2002;219:139–50.
34. Bergen HR 3rd, Ajtai K, Burghardt TP, Nepomuceno AI, Muddiman DC. Mass spectral determination of skeletal/cardiac actin isoform ratios in cardiac muscle. Rapid Commun Mass Spectrom 2003;17:1467–71.
35. Nepomuceno AI, Muddiman DC, Bergen HR, Craighead JR, Burke MJ, Caskey PE, et al. Dual electrospray ionization source for confident generation of accurate mass tags using liquid chromatography Fourier transform ion cyclotron resonance mass spectrometry. Anal Chem 2003;75:3411–8.
36. Kryschenko YK, Seidel SR, Muddiman DC, Nepomuceno AI, Stang PJ. Coordination-driven self-assembly of supramolecular cages: heteroatom-containing and complementary trigonal prisms. J Am Chem Soc 2003;125:9647–52.
37. Chalmers MJ, Quinn JP, Blakney GT, Emmett MR, Mischak H, Gaskell SJ, et al. Liquid chromatography-Fourier transform ion cyclotron resonance mass spectrometric characterization of protein kinase C phosphorylation. J Proteome Res 2003;2:373–82.
38. Belov ME, Zhang R, Stritmatter EF, Prior DC, Tang K, Smith RD. Automated gain control and internal calibration with external ion accumulation capillary liquid chromatography-electrospray ionization-Fourier transform ion cyclotron resonance. Anal Chem 2003;75:4195–205.
39. Lee SW, Berger SJ, Martinovic S, Pasa-Tolic L, Anderson GA, Shen Y, et al. Direct mass spectrometric analysis of intact proteins of the yeast large ribosomal subunit using capillary LC/FTICR. Proc Natl Acad Sci U S A 2002;99:5942–7.
40. Bergen HR, Zeldenrust SR, Butz ML, Snow DS, Dyck PJ, Dyck JB, et al. Identification of transthyretin variants by sequential proteomic and genomic analysis. Clin Chem 2004;50:1544–52.
41. Chowdhury SK, Katta V, Chait BT. An electrospray-ionization mass spectrometer with new features. Rapid Commun Mass Spectrom 1990;4:81–7.
42. Senko MW, Beu SC, McLafferty FW. Determination of monoisotopic masses and ion population for large biomolecules from resolved isotopic distributions. J Am Soc Mass Spectrom 1995;6:229–33.
43. Rockwood AL, Van Orden SL. Ultrahigh-speed calculation of isotope distribution. Anal Chem 1996;68:2027–30.
44. Sass JO, Nakanishi T, Sato T, Sperl W, Shimizu A. *S*-Homocysteinylation of transthyretin is detected in plasma and serum of humans with different types of hyperhomocysteinemia. Biochem Biophys Res Commun 2003;310:242–6.
45. Getz EB, Xiao M, Chakrabarty T, Cooke R, Selvin PR. A comparison between the sulfhydryl reductants tris(2-carboxyethyl)phosphine and dithiothreitol for use in protein biochemistry. Anal Biochem 1999;273:73–80.
46. Han JC, Han GY. A procedure for quantitative determination of tris(2-carboxyethyl)phosphine, an odorless reducing agent more stable and effective than dithiothreitol. Anal Biochem 1994;220:5–10.
47. Zubarev RA, Demirev PA, Hakansson P, Sundqvist BUR. Approached and limits for accurate mass characterization of large biomolecules. Anal Chem 1995;67:3793–8.
48. Horn DM, Zubarev RA, McLafferty FW. Automated resolution and interpretation of high resolution electrospray mass spectra of large molecules. J Am Soc Mass Spectrom 2000;11:320–32.
49. Ando Y, Almeida M, Ohlsson PI, Ando E, Negi A, Suhr O, et al. Unusual self-association properties of transthyretin Y114C related to familial amyloidotic polyneuropathy: effects on detection and quantification. Biochem Biophys Res Commun 1999;261:264–9.